The Influence of Phosphorous and High Temperature Annealing on the Nanostructures of 3C-SiC.

I J van Rooyen[1, 2, 4], J H Neethling [2], A Henry[3], E Janzén[3]
PBMR, Fuel Design
1279 Mike Crawford Avenue, Centurion, 0046, South Africa
phone: +27-07-7449015, isabel.vanrooyen@pbmr.co.za

[1]*Fuel Design, PBMR, 1279 Mike Crawford Avenue, Centurion, 0046, South Africa*

[2]*Department of Physics, Nelson Mandela Metropolitan University, PO Box 77000, Port Elizabeth, 6031, South Africa.*

[3]*Department of Physics, Chemistry and Biology, Semiconductor Materials, Linköping University, Linköping , 58183, Sweden,*

[4]*National Laser Centre, CSIR, P.O. Box 395, Pretoria 0001, South Africa.*

Abstract – *The integrity and property behaviour of the SiC layer of the TRISO coated particle for high temperature reactors (HTR) are very important. The SiC is the main barrier for gaseous and metallic fission product release. An investigation was proposed to determine the effect that different Si isotopes may have on the SiC crystal structure during the CVD manufacturing process and after transmutation due to irradiation.* ^{30}Si *transmutes to phosphorous (*^{31}P*) and other transmutation products during irradiation, which may affect the integrity of the SiC layer. This study describes the work done on unirradiated SiC, but the SiC samples were prepared with varying phosphorous levels to "simulate" the presence of P due to transmutation. Phosphorous-doped 3C-SiC layers were deposited on Si (100) substrates using the concept of the hot wall chemical vapour deposition with silane (*SiH_4*) and propane (*C_3H_8*) as precursors diluted in hydrogen (*H_2*). Propane was introduced in the reactor chamber prior to the silane addition during the heating-up cycle to prepare a thin layer of SiC on the silicon substrate. This was to ensure epitaxial growth of mono-crystalline layers once silane is added at the growth temperature. However by changing growth procedures polycrystalline layers were also obtained. Phosphorus doping of the layers was done during epitaxy using tertiary butyl phosphine (TBP) (*$C_4H_9PH_2$*) as a donor source, the doping level was varied between* $1.1x10^{15}$ *and* $1.2x10^{19}$ *atom/cm*^{3}*. The P-doped SiC layers were characterized after high temperature annealing from 1600 ºC to 2100 ºC using five techniques namely X-ray diffraction (XRD), secondary ion mass spectrometry (SIMS), scanning electron microscopy (SEM), transmission electron microscopy (TEM) and high resolution transmission electron microscopy (HRTEM). The HRTEM micrograph of the decomposition of SiC at 2100 ºC are shown and discussed. Nanotubes were not identified during the TEM and HRTEM analysis although graphitic structures were identified. The preliminary conclusion reached is that the P-content at these experimental levels (*$1.1x10^{15}$ *-* $1.2x10^{19}$ *atom/cm*^{3}*) does not have a significant influence on the nanostructure of SiC at high temperatures without irradiation.*

I. INTRODUCTION

The integrity and property behaviour of the SiC layer of the TRISO coated particle for high temperature reactors (HTR) are very important. The SiC is the main barrier for gaseous and metallic fission product release. An investigation was proposed to determine the effect that different Si isotopes may have on the SiC crystal structure during the CVD manufacturing process and after transmutation due to irradiation. ^{30}Si transmutes to phosphorous (^{31}P) and other transmutation products

during irradiation, which may affect the integrity of the SiC layer. This study describes the work done on unirradiated SiC, but the SiC samples were prepared with varying phosphorous levels to "simulate" the presence of P due to transmutation. Heinisch et al. [1] reported that 36 appm P are produced by neutron irradiation-induced transmutation in a modular pebble bed reactor (265 MWth, total neutron flux 1.25×10^{14} n/cm^{2}s for 10 full power years (4.4 displacements per atom (dpa)). This amounts to 8.2 appm/dpa phosphorous.

Calculations of material activation due to neutrons were done by the PBMR's Nuclear Engineering Analysis (NEA) group using European Activation System-2007 (EASY) comprising of the EAF-2007 nuclear data and the FISPACT-2007 inventory code. These calculations were done for the different isotopic compositions of SiC as part of the Fuel Design study, but only the results for the natural Si-isotopic composition (92.2% ^{28}Si, 4.6% ^{29}Si, and 3.1% ^{30}Si) for SiC are described in this paper. Density of SiC used is 3.20 g/cm^3 and the total volume of SiC layer irradiated is 7.13×10^{-05} cm^3. The fuel residence time in the reactor core was determined by VSOP and is 925 days, meaning that one cycle through the PBMR will take in average 152.16 days (925/6). Thus the irradiation time used for this calculation is for the fuel residence time of 925 days and is applicable to the 6 passes for the 400 MWth PBMR design. The cooling period applied for this activation is 30 days [2]. These calculations revealed that 10 appm P are produced by neutron irradiation-induced transmutation under PBMR conditions.

I. MATERIALS AND CHARACTERIZATION METHODS

II.A. Materials

Phosphorous-doped 3C-SiC layers were deposited, at the Linköping University's (LiU) facility, on Si (100) substrates using the concept of the hot wall chemical vapour deposition with silane (SiH_4) and propane (C_3H_8) as precursors diluted in hydrogen (H_2). Propane was introduced in the reactor chamber prior to the silane addition during the heating-up cycle to prepare a thin layer of SiC on the silicon substrate. This was to ensure epitaxial growth of mono-crystalline layers once silane is added at the growth temperature. However by changing growth procedures polycrystalline layers were also obtained. Phosphorus doping of the layers was done during epitaxy using tertiary butyl phosphine (TBP) ($C_4H_9PH_2$) as a donor source [3]. The SiC deposition temperature varies between 1210 ºC and 1320 ºC for the thirteen samples manufactured. Fig. 1 shows the growth conditions of polycrystalline batch X364 in the horizontal hot walled CVD reactor.

Sample MH149 was prepared with hydrochloric acid (HCl) added and the process is described as "chloride based epitaxy". Pedersen et al. [4] shows in a previous study that the optimum level of Si to Cl ratio for this process is 3, in order to avoid etching of the epilayer.

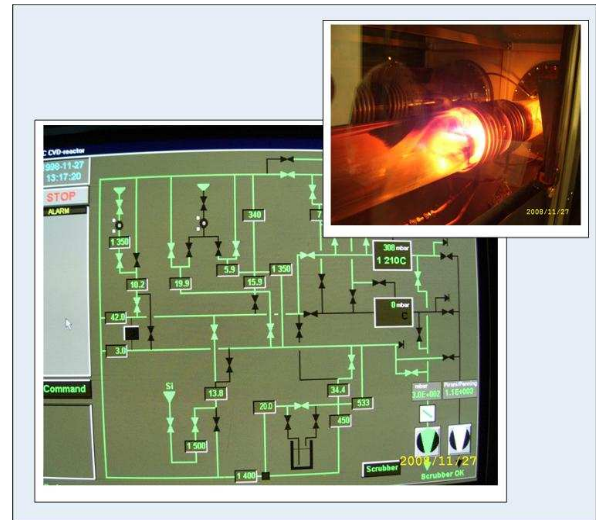

Fig. 1: Polycrystalline 3C-SiC batch X364 growing in the LiU horizontal hot walled CVD reactor at 1210 ºC.

II.B. Characterization Methods

The P-doped SiC layers were characterized after high temperature annealing from 1600ºC to 2100ºC using various techniques. The LiU samples were further divided in smaller samples and the specific characterization work executed on the sub-samples is determined and a typical example is schematically shown in Fig. 2.

Annealing was performed in a resistively heated Webb 89 vacuum furnace supplied by R.D. Webb Company USA. The samples were loaded in graphite or ceramic holders at room temperature and heated to the required temperature at a rate of 25ºC per minute. After completion of annealing at the required holding time and temperature, the samples were furnace-cooled to room temperature. As the Linkoping samples were SiC grown on Si-wafers, argon annealing atmosphere were chosen to ensure that the vaporized silicon be removed from the sample surfaces to prevent contamination of the SiC samples itself. However, due to the furnace maximum temperature limitations, the annealing of sample X377CB at 2100°C were conducted under vacuum for 10 minutes only. The rest of the samples were annealed under argon for 1h and 0.5h for the 1600°C and 2000°C cycles respectively.

The results of only five techniques namely X-ray diffraction (XRD), secondary ion mass spectrometry (SIMS), scanning electron microscopy (SEM), transmission electron microscopy (TEM) and high resolution transmission electron microscopy (HRTEM), are briefly described in this paper. The results obtained from the other techniques like the Atomic Force Microscopy (AFM) and Fourier Transformed Infrared (FTIR) will be described in separate articles at a later stage. The basic principles of the specific five techniques are not described in this paper.

It needs to be noted that although different structure morphologies were found and briefly discussed in this paper, the relevant subsamples used for the TEM observations, exhibited similar morphologies. The annealing studies on X364 subsamples which show globular structures were therefore not considered in reaching conclusions in this study. A large number of TEM micrographs (>250) were analyzed for this study to facilitate the conclusions reached.

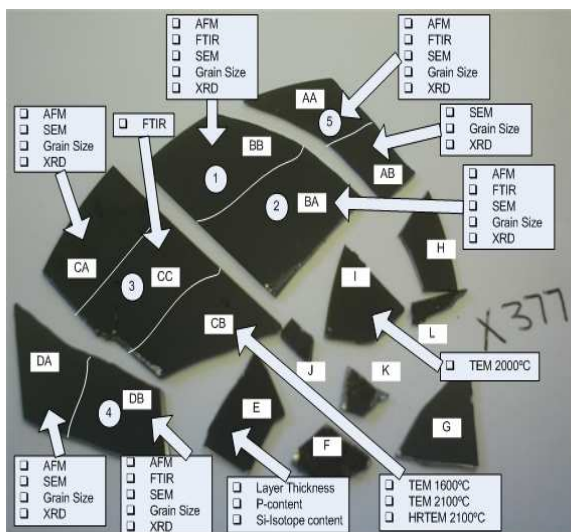

Fig. 2: Typical example of the schematic presentation of LiU P-doped polycrystalline X377 sample and characterization identification.

III. RESULTS AND DISCUSSION

III.A. X-Ray Diffraction

X-Ray diffraction measurements were conducted using the Philips PW1729 diffractometer at the LiU Physics department and the Philips PW1840 diffractometer at NMMU. The diffractograms for all samples showed the 3C-SiC phase grown on Si (100). A typical diffractogram of the single crystal sample X361 measurement is shown in the diffractogram (2θ-scan) in Fig. 3 and were used to identify the SiC phase and the orientation of the epilayer. The epilayer is grown heteroepitaxially and only the (h00) peaks are visible since there is a preferred orientation.

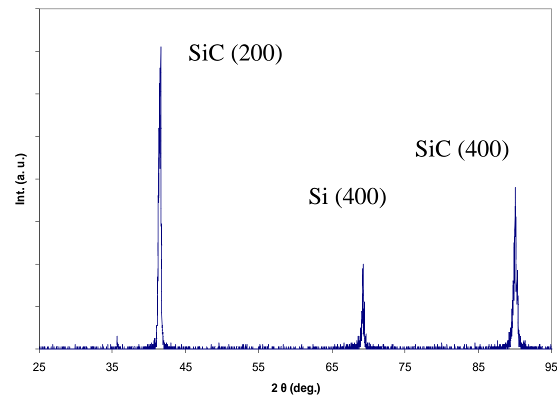

Fig. 3: Batch 361 XRD diffractogram of the 3C-SiC grown on Si (100). The epilayer is grown heteroepitaxially and only the (h00) peaks are visible since there is a preferred orientation.

III.B. Chemical Analysis

The P-content in selected LiU P-doped prior to annealing was measured by the Evans Analytical Group (EAG), USA, using SIMS with a detection limit of $1x10^{13}$ at/cm^3 and these measurements are shown in Table 2. The doping level varied between $1.1x10^{15}$ - $1.2x10^{19}$ at/cm^3. Sample X377 have the highest doping level at $1.2x10^{19}$ at/cm^3 and was therefore chosen to discuss further in this paper.

The PBMR calculated value for the typical PBMR reactor yields a P concentration of $9.8x10^{17}$ at/cm^3. The P-doping levels of the selected samples indicated in Table 2, showed that these LiU prepared samples are relevant to the PBMR conditions as it gives a representative P concentration spread around typical PBMR conditions. This phosphorous concentration is also in the same order found by neutron-transmutation studies done by Baranov et al. [5] for a neutron dose of ~ 1x 10^{20} cm^{-2} for ^{30}Si enriched SiC. Wellmann [6] found that P-doping concentrations of up to $1.3x10^{18}$ at/cm^3 were achieved and further suggested that much higher doping levels are achievable. The work presented in this paper showed achieved concentrations up to $1.19x10^{19}$ at/cm^3.

Hendriks et al. [7] found that for low doping concentrations, the P atoms will be trapped at the grain boundaries, but that for higher doping concentrations only a small fraction of P atoms will be trapped at the grain boundaries and therefore only a small depleted zone next to the grain boundaries are expected. The SIMS analysis of the LiU samples was done on bulk areas and therefore no detail

profile is available to confirm or reject this statement.

Sample No.	EAG SIMS P concentration (at/cm^3)		
	Analysis 1	Analysis 2	Average
X380-C	6.46×10^{18}	6.72×10^{18}	6.59×10^{18}
X377-E	1.20×10^{19}	1.18×10^{19}	1.19×10^{19}
X383-BA	5.23×10^{17}	5.45×10^{17}	5.34×10^{17}
X387-BA	5.36×10^{15}	5.35×10^{15}	5.36×10^{15}
X382-G	1.65×10^{18}	1.57×10^{18}	1.61×10^{18}
X391-B	1.08×10^{15}	1.13×10^{15}	1.11×10^{15}
X392-B	1.75×10^{15}	1.71×10^{15}	1.73×10^{15}
X393-B	6.68×10^{15}	6.74×10^{15}	6.71×10^{15}

Table 2: Bulk SIMS Analysis of P in SiC.

III.C. Scanning Electron Microscopic Evaluation

A XL30 Philips SEM at NMMU was used to investigate the top surface morphology of the samples prepared at LiU and to determine the grain sizes.

The grain sizes of selected samples from X364, X377, X380 and X383 were determined using the Heyn Lineal Intercept method in accordance with ASTM E112 [8]. The SEM micrographs in Fig. 4 show globular top surface structure for sample X364 and the grain size measurement shows a large variation in grain size, which probably indicated a large variance in the SiC deposition temperature. The grain sizes of sample X377 showed approximately even average sizes and fairly homogeneous morphologies (Fig. 5).

From the grain size determination schematically presented in Fig. 6, it is shown that grain sizes of the P-doped polycrystalline samples are fairly evenly sized whereas large grain size variances are visible for the un-doped sample X364. This fairly homogeneous grain size distribution of the P-doped samples, showed that the deposition temperature were in a narrow range as in contrast with those of sample X364. During the preparation of sample X364 it was also further observed that the substrate sample was located near the input end of the chamber and that the temperature in that region was most probably higher as reported for this growth. The presence of molten Si substrate was observed during the removal of the sample which is also an indication of much higher temperature. The yellow optical color of the top edge of sample X364 also indicate that the substrate temperature for sub-samples X364AB and X364AC may have been higher as the recorded 1210 ºC. Deductions from work by Chin et al. [9] showed that the yellow optical color may indicate a higher substrate temperature.

Fig. 4: Average grain size distribution in the LiU P-doped polycrystalline 3C-SiC sample X364.

López-Honorato et al. [10] indicated that the top surface changed from a globular to a faceted structure as stoichiometry improves. Fig. 7 is included to show the difference between typical globular and faceted top surface structures. The stoichiometry of these samples is however not confirmed at time of this study. The effect of deposit temperature on these three examples are not as clear as described by Lee et al. [11] and Chin et al. [9], but it is important to notice that the doping levels are varying and therefore the manufacturing conditions are different for each sample as well. It is recommended that these morphologies together with the rest of the thirteen LiU samples be investigated in conjunction with the respective manufacturing parameters.

Fig. 5: Average grain size distribution in the LiU P-doped polycrystalline 3C-SiC sample X377.

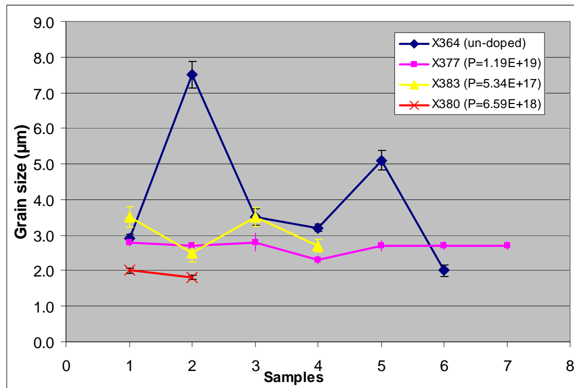

Fig. 6: Schematic presentation of the grain size distribution measured on different positions on the sample. The grain size distribution curve of un-doped polycrystalline sample X364 is shown for comparison

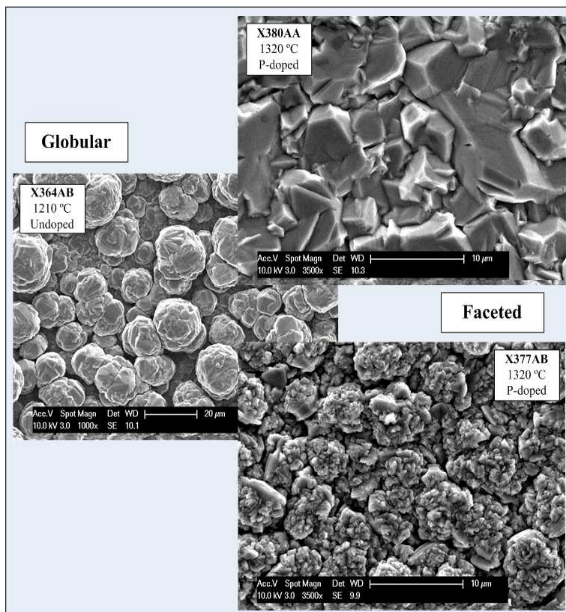

Fig. 7: SEM micrographs showing the difference between typical globular and faceted top surface structures.

III.D. Transmission Electron Microscopic Evaluation

A 200 kV Philips CM20 transmission electron microscope was used for the TEM analysis. A large amount of TEM micrographs were taken and evaluated to determine the effect of temperature and P-doping level on the nanostructures of 3C-SiC. Only selected images are shown in this paper as it represents the typical results obtained from the full TEM evaluation.

High resolution TEM images were acquired using a JEOL 2200MCO aberration corrected (S)TEM operated at 200kV with an in-column omega filter (Oxford University).

The single crystal LiU 3C-SiC samples (P concentration from 0 to 6.71E+15 at/cm^3) were annealed at 1600 ºC and 2000 ºC. The TEM evaluation of these samples showed that no phase transformation, no nanotubes and no decomposition were observed for these P-doping levels up to an annealing temperature of 2000 ºC.

The annealing of the polycrystalline LiU 3C-SiC samples were done at 1600 ºC, 2000 ºC and 2100 ºC respectively where phase transformation from 3C- to 6H-SiC were observed for samples X364 (un-doped) and X377 (highest P-doped sample) at 2000 ºC. As both these samples showed a phase transformation, it indicates that the P-doping level is not a contributing fact towards this phase transformation, but it is temperature dependant. Fig. 8 and Fig. 9 show the bright field (BF) TEM image and corresponding selected area diffraction (SAD) of the samples X364 and X377 after annealing at 1600 ºC and 2000 ºC respectively. Fig. 10 shows the BF TEM image and SAD of the sample X377CB after annealing at 2100 ºC. Evidence of decomposition of SiC is clearly visible. The diffraction ring pattern in Fig 10 shows that the SiC transformed to polycrystalline graphite. The first four rings of graphite 002, 101, 004 and 112, are visible. No nanotubes were observed in any of the polycrystalline LiU samples.

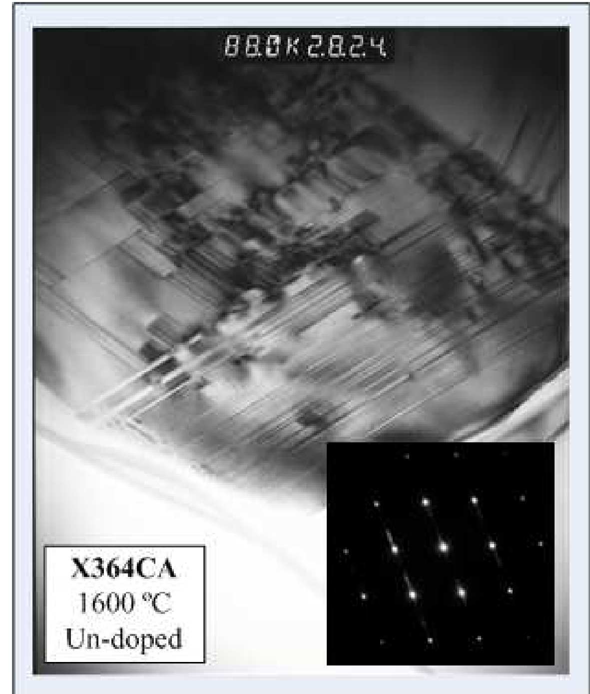

Fig. 8: Bright Field TEM micrograph and SAD pattern of sample X364CA after annealing at a temperature of 1600°C. The SAD is consistent with the cubic 3C-SiC phase with the beam along the <110> direction. The streaks in the SAD are due to the thin twin platelets visible in the bright-field TEM image.

The HRTEM image in Fig. 11 shows the SiC-graphite interface region of sample X377CB after annealing at 2100°C. Randomly orientated graphite lamella which has the (002) parallel to the electron beam, display the typical HRTEM fringe image of the basal planes. The SiC-graphite interface region and the graphite lamella are shown in Fig. 12 at a higher magnification.

Fig. 9: Bright Field TEM micrograph and SAD of sample X377I after annealing at a temperature of 2000°C. The SAD indicates that a phase transformation to 6H-SiC hexagonal phase occurred. The beam is along the <100>.

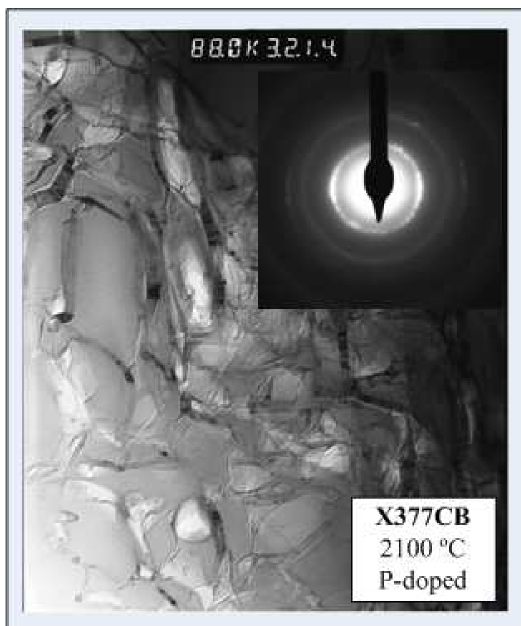

Fig. 10: Bright Field TEM micrograph and SAD of sample X377CB after annealing at a temperature of 2100°C. The SAD shows the four rings of the graphite namely 002, 101, 004 and 112.

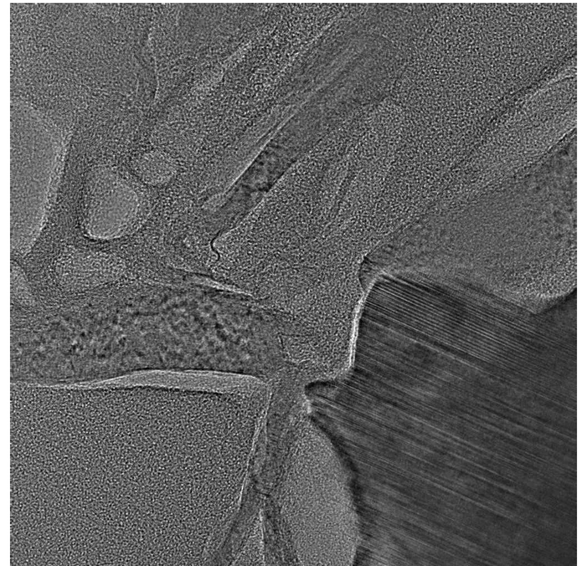

Fig. 11: HRTEM image (250 000x) of the SiC-graphite interface region of sample X377CB after annealing at 2100°C.

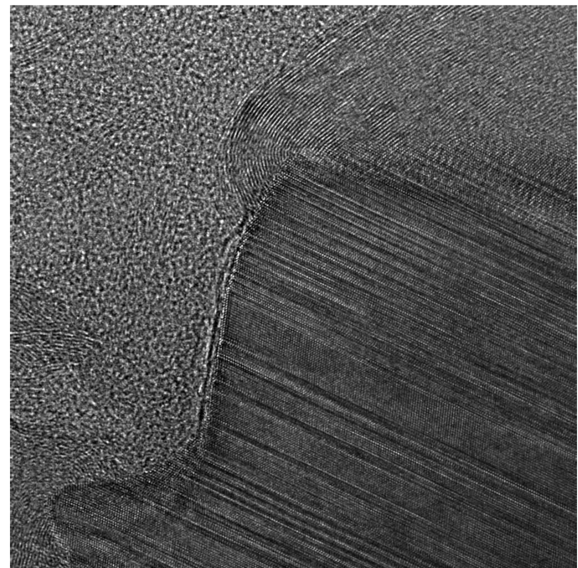

Fig. 12: HRTEM image of sample X377CB after annealing at a temperature of 2100°C showing the basal planes in the graphite lamella at higher magnification (800 000x).

IV. CONCLUSIONS

The preliminary conclusion reached is that the P-content at these experimental levels (1.1×10^{15} atom/cm^3 -1.2×10^{19} atom/cm^3) does not have a significant influence on the nanostructure of SiC after annealing at high temperatures without irradiation.

Although phase transformations from 3C- to 6H-SiC were observed after annealing at 2000 ºC, it is not attributed to the P-doping concentrations.

Decomposition of the SiC is only observed at 2100ºC annealing temperature and no nanotubes were identified during the TEM and HRTEM analysis although graphitic structures were identified.

V. RECOMMENDATIONS

It is recommended that the morphologies and stoichiometry of the three samples mentioned in this paper together with the rest of the thirteen LiU samples be investigated in conjunction with the respective manufacturing conditions and influence of the P-doping on the resistivity of SiC. It is also recommended that the influence of P-doping level on the heat conductivity and mechanical properties of SiC be determined.

ACKNOWLEDGEMENTS

This research was sponsored by PBMR's Fuel Optimization Technology Programme. The use of the NMMU and PBMR Fuel Development Laboratory facilities are gratefully acknowledged. Johannes Mahlangu (PBMR), Ellen Nquma (PBMR), Jaco Olivier (NMMU) and Jacques O' Connell (NMMU) are thanked for the annealing operations. The HRTEM images were produced by Dr Sarah Haigh at Oxford University.

REFERENCES

[1] H. L. Heinisch, L.R. Greenwood, W. J. Weber, R. E. Williford, Displacement damage in silicon carbide irradiated in fission reactors, Journal of Nuclear Materials, 327, (2004) 175-181

[2] S. Maage, Inventory products of SiC layer under PBMR conditions, PBMR Design Information Transmittal DIT001316, (2009)

[3] A. Henry, E Janzén, Epitaxial growth and characterization of phosphorous doped SiC using TBP as precursor, Materials Science Forum Vols. 483-485 (2005) 101-104

[4] H. Pedersen, Chloride-based Silicon Carbide CVD, Linkoping Studies in Science and Technology, Dissertation No. 1225, (2008)

[5] P. G. baraniv, B. Ya. Ber, I. V. Ilyin, A. N. Ionov, E. N. Mokhov, M. V. Muzafarova, M. A. Kalieevskii, P. S. Kopév, A. K. K Kalieevskii, O. N. Godisov, I. M. Lazebnik, Pecularities of neutron-transmutation phosphorous doping of ^{30}Si enriched SiC crystals: Electron paramagnetic resonance study, Journal of Applied Physics, 102, 063713 (2007)

[6] P. J. Wellmann, Additional pipework opens up transistor applications for SiC, http://compoundsemiconductor.net/articles/magazine/11/3/3/1 date of access 2007/01/17 (2005)

[7] M. Hendriks, S. Radelaar, T. H. de Keijser and R. Delhez, Morphology and resistivity of CVD polycrystalline silicon layers containing carbon, EDP Sciences, http://dx.doi.org/10.1051/jphyscol:1982141 (1982)

[8] ASTM E112-96 Standard Test Methods for Determining Average Grain Size, (Re-approved 2004)

[9] J. Chin, P. K. Gantzel, R. G. Hudson, The structure of chemical vapor deposited silicon carbide, Thin Solid Films, 40 57-72 (1977)

[10] E. López-Honorato, P.J. Meadows, J. Tan, and P. Xiao, Control of stoichiometry, microstructure, and mechanical properties in SiC coatings produced by fluidized bed chemical vapor deposition, J. Mater. Res., 23, No. 6, (2008)

[11] K. S. Lee, J. Y. Park, W. Kim, G. W. Hong, Effect of microstructure of SiC layer on the indentation properties of silicon carbide-graphite system fabricated by LPCVD method, Journal of Materials Science letters, 20 1229-1231 (2001)